The cell parameters of the arfvedsonite–eckermannite series, with observations on the MgO and total iron content of amphiboles

D. R. C. KEMPE

Department of Mineralogy, British Museum (Natural History),
Cromwell Road, London, S.W.7

SUMMARY. The cell parameters of 35 members of the arfvedsonite–eckermannite series and catophorites (17 from the literature, 18 newly determined) are presented and an attempt made to relate them to chemical composition. In general, all parameters (including β, obtuse) decrease from arfvedsonite to eckermannite, but for different reasons: a, b, and β (very slightly) as the Mg:Fe^{2+} ratio and F increase; c as Fe^{3+} decreases. The apparent decrease in a and b with high Li is coincidental, due to its strong correlation with F, which varies inversely with (OH). In addition, b is increased by high Ca and slightly reduced by high Al.

Also, the empirical and calculated curves relating MgO and total iron as Fe_2O_3 (weight %) with the Mg ratio, 100 Mg/(Mg+Fe^{2+}+Fe^{3+}+Mn), for all amphibole groups are given, as a rapid method of obtaining an estimate of the Mg ratio.

The full lists of possible hkl values for an arfvedsonite and an eckermannite are enumerated up to 45° 2θ, Cu-$K\alpha$, to illustrate the difficulty in indexing X-ray photographs and diffractometer charts of this group.

THE cell parameters of fourteen analysed riebeckitic arfvedsonites from the Younger Granites of Nigeria have been determined by Frost (1963). These amphiboles are, however, very low in MgO and rich in Li_2O (and also ZnO and F), and are in general chemically similar. In order to extend coverage of the cell dimensions to as many as possible of the arfvedsonite–eckermannite series (as defined by Deer et al. (1963) and with the general formula for the intermediate member:

$$Na_{2.5}Ca_{0.5}(Fe^{2+},Li,Mg,Fe^{3+},Al)_5[Si_{7.5}Al_{0.5}O_{22}](OH,F)_2)$$
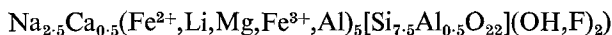
the parameters have been determined on amphiboles from a wide variety of parageneses. These include four analysed arfvedsonites and one catophorite from the Kangerdlugssuaq alkaline intrusion, East Greenland; a blue arfvedsonitic magnesio-riebeckite from an alkali schist from Tanzania; an arfvedsonite from an ejected plutonic block from Ascension Island; and the eckermannite ('széchenyiite') from the jadeite rock of Tawmaw, Burma. A further eight members of the series, for which no analyses are available but of which an estimate of the Mg ratio has been obtained by the method described below, have also been measured. In addition, the dimensions of an arfvedsonite from Tunugdliarfik, Greenland, given by Kawahara (1963; also ASTM 14-633), and of a manganoan arfvedsonite (juddite) from North Tirodi, and an eckermannite from Goldongri, India (Nayak and Neuvonen, 1963), have been included, whilst the parameters of mboziite, which may be regarded as a catophorite of

TABLE I. *Description of specimens*

No. of specimen	Wt %				Mg or (Mg+Li) ratio	Reference number, description, locality, and source
	CaO	MgO	Li₂O	(total) Fe₂O₃		
1	2·67	0·07	n.d.	37·28	0·4	69525 — Arfvedsonite. Ascension Island. J. R. Cann, unpub.; anal. J. H. Scoon.
2	1·19	0·46	n.d.	39·01	1·1	— Arfvedsonite. Nunarsuatsiak, Tunugdliarfik, Greenland. Kawahara (1963); ASTM 14-633.
3	4·27	0·34	n.d.	38·21	1·6	A.16 — Arfvedsonite. Nigeria. Borley (1963).
4	7·54	0·83	n.d.	35·10	4·4	— Mboziite (catophorite). Darkainle, Somali Republic. Brock et al. (1964).
5	2·88	0·03	0·42	36·44	5·7	A.3 — Arfvedsonite. Nigeria. Borley (1963).
6	1·74	0·07	0·46	38·55	6·2	A.5 — Arfvedsonite. Nigeria. Borley (1963).
7	5·78	1·24	n.d.	33·92	6·4	— Mboziite (catophorite). Mbozi, SW. Tanzania. Brock et al. (1964).
8	0·87	0·05	0·53	39·03	7·1	A.2 — Arfvedsonite. Nigeria. Borley (1963).
9	0·90	0·16	0·51	36·20	7·7	A.7 — Arfvedsonite. Nigeria. Borley (1963).
10	1·25	1·52	0·06	32·92	8·6	EG 2046 — Arfvedsonite. Kangerdlugssuaq, E. Greenland. Kempe and Deer (in press).
11	0·49	0·03	0·65	36·15	8·7	A.15 — Arfvedsonite. Nigeria. Borley (1963).
12	2·22	0·44	0·52	37·98	8·8	A.4 — Arfvedsonite. Nigeria. Borley (1963).
13	1·79	0·03	0·67	36·67	8·9	A.6 — Arfvedsonite. Nigeria. Borley (1963).
14	0·88	0·05	0·74	37·37	8·9	A.13 — Arfvedsonite. Nigeria. Borley (1963).
15	1·02	0·05	0·99	36·53	12·6	A.9 — Arfvedsonite. Nigeria. Borley (1963).
16	1·95	0·42	0·97	35·89	14·1	A.8 — Arfvedsonite. Nigeria. Borley (1963).
17	0·64	0·30	1·16	35·99	15·8	A.12 — Arfvedsonite. Nigeria. Borley (1963).
18	n.d.	n.d.	n.d.	31·2	(18)	BM 1961, 236 — Arfvedsonite. Khibina, Kola Peninsula.
19	0·31	0·13	1·76	34·58	21·6	A.14 — Arfvedsonite. Nigeria. Borley (1963).
20	0·20	0·04	2·20	32·94	25·4	A.1 — Arfvedsonite. Nigeria. Borley (1963).
21	0·90	5·00	0·09	26·99	25·4	EG 4666 — Arfvedsonite. Kangerdlugssuaq, E. Greenland. Kempe and Deer (in press).

TABLE I (cont.)

No. of specimen	Wt. %				Mg or (Mg+ Li) ratio	Reference number, description, locality and source
	CaO	MgO	Li$_2$O	(total) Fe$_2$O$_3$		
22	5·83	5·53	0·01	28·33	26·9	EG 1397. Catophorite. Kangerdlugssuaq, E. Greenland. Kempe and Deer (in press).
23	3·77	7·44	0·02	22·84	37·3	EG 4582. Magnesio-arfvedsonite. Kangerdlugssuaq, E. Greenland. Kempe and Deer (in press).
24	3·59	9·75	0·02	20·21	46·9	EG 4789. Magnesio-arfvedsonite. Kangerdlugssuaq, E. Greenland. Kempe and Deer (in press).
25	n.d.	n.d.	n.d.	17·9	(53)	BM 1932, 104 (2). Magnesio-arfvedsonite. Lulu Kop, Palabora, E. Transvaal.
26	0·46	10·03	n.d.	16·11‡	55·2	— Manganoan arfvedsonite (juddite). North Tirodi, India. Nayak and Neuvonen (1964).
27	n.d.	n.d.	n.d.	16·0	(59)	B 288. Magnesio-arfvedsonite. Loyne, Borolan, Scotland.
28	n.d.	n.d.	n.d.	16·0	(59)	N 82. Magnesio-arfvedsonite. Fen area, Norway.
29	n.d.	n.d.	0·88	14·9‡	(62)	BM 1955, 122. Manganoan arfvedsonite (juddite). Chikla, India.
30	2·91	13·52	n.d.	15·88	62·7	RL 523. Magnesioriebeckite. SW. Tanzania. Kempe (1968)
31	n.d.	n.d.	n.d.	13·6	(66)	MW 325. Magnesio-arfvedsonite. Namangali, Malawi.
32	n.d.	n.d.	0·62	13·6	(66)	BM 1951, 408 (21). Eckermannite. Norra Kärr, Sweden.
33†	n.d. [0·31]	n.d. [9·13]	0·95 [1·15]	12·6 [11·00]	(69) [68·1]	BM 1949, 151. Eckermannite. Norra Kärr, Sweden.
34	4·95	17·75	n.d.	9·37‡	78·9	— Eckermannite. Goldongri, India. Nayak and Neuvonen (1964).
35†	[1·40]	[18·56]	n.d.	[3·86]	[90·6]	48639. Eckermannite (széchenyiite). Tawmaw, Burma.

n.d.: not determined.

Values of Mg ratio in parentheses denote estimates from the total iron curve (fig. 3).

† The values of oxides and Mg ratio in brackets are those given by Deer et al. (1963, table 57, analyses 1 and 3). ‡ Includes MnO and Mn$_2$O$_3$.

Nos. 18, 25, and 27–33: total iron (as Fe$_2$O$_3$), Li$_2$O, (and MnO) determinations by A. J. Easton.

extreme composition, from Mbozi, Tanzania, and Darkainle, Somali Republic, have been computed from the *d* spacings given by Brock *et al.* (1964). Members of the catophorite–magnesiocatophorite series have been included to the extent mentioned above, since they form a parallel series very closely related to the arfvedsonite–eckermannite group.

Deer *et al.* (1963) present each of the amphibole groups as a series of varying 100 Mg/(Mg+Fe^{2+}+Fe^{3+}+Mn) (atomic) ratio, between end-members of fixed composition. The cell parameters of the arfvedsonite–eckermannite series are related to the Mg ratio and illustrate a progressive decrease from the iron-rich to the magnesium-rich ends. In the case of amphiboles rich in Li$_2$O, it is necessary to modify the ratio to
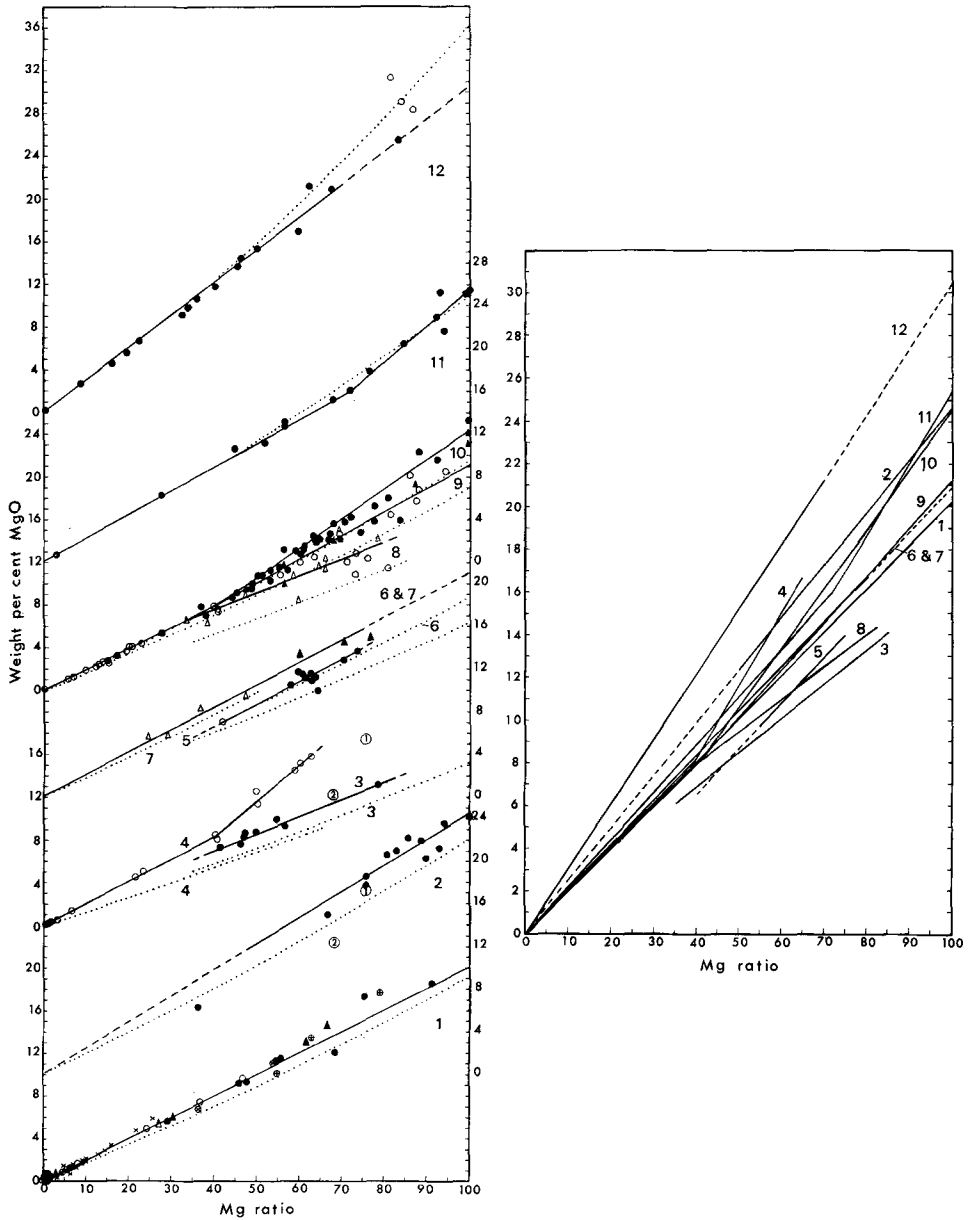
FIGS. 1 and 2: FIG. 1 (left). Weight % MgO or (MgO+Li₂O) plotted against Mg or (Mg+Li) atomic ratio (100 Mg/(Mg+Fe²⁺+Fe³⁺+Mn) or 100 (Mg+Li)/(Mg+Li+Fe²⁺+Fe³⁺+Mn)) for the analyses of various amphiboles series given by Deer *et al.* (1963) and others; the calculated curve is shown as a dotted line for each series: *Line 1*, ● arfvedsonite–eckermannite series (Deer *et al.*, 1963, table 57), ▲ catophorites (Deer *et al.*, 1963, table 56), ○ arfvedsonite–eckermannite series (Kempe and Deer, in press), △ catophorite (Kempe and Deer, in press), ✕ riebeckitic arfvedsonites (Borley, 1963, tables II and III), ⊗ magnesio-arfvedsonites (McKie, 1966, p. 279), and ⊕ others. *Line 2*,

include Li (see Deer *et al.*, 1963, p. 366), since it is now generally accepted that Li normally substitutes for Mg.

Compositional considerations. In table I are listed the amphiboles investigated by the present and previous writers, in order of increasing Mg ratio. In order to obtain estimates of the Mg ratio of the eight amphiboles for which no analyses are available, the MgO (wt. %) and total iron, as Fe_2O_3, values were plotted against Mg ratio for all the analyses of members of the arfvedsonite–eckermannite and the catophorite–magnesiocatophorite series given in Deer *et al.* (1963, tables 56 and 57), together with the others investigated by the writer. It was found that for the arfvedsonite–eckermannite series, near-linear relations were obtained for MgO (fig. 1, line 1) and for total iron as Fe_2O_3 (fig. 3, line 1), there being two exceptions (Deer *et al.*, 1963, table 57, analyses 2 and 3), discussed below. In the case of the Li-rich Nigerian amphiboles (Borley, 1963), $(MgO+Li_2O)$ is plotted against $100(Mg+Li)/(Mg+Li+Fe^{2+}+Fe^{3+}+Mn)$, Li_2O being corrected for its different equivalent weight (MgO, 40·3; $LiO_{\frac{1}{2}}$, 14·9; giving a factor of 2·705). The resultant values also plot well on the curve, the greatest ratio discrepancy (3·5 %) being in the case of A.1. The Nigerian amphiboles have high total iron values, however, due to their high content of Fe_2O_3 (averaging 13·0 % in those containing *c*. 1 % Li_2O or more, as compared with an average of 10·3 % in amphiboles of comparable Mg ratio analysed by the writer and others). This results from the substitution of Fe^{3+} for Fe^{2+} necessary to maintain electron charge balance, thus: $MgFe^{2+} \rightleftharpoons LiFe^{3+}$.

Only four catophorite analyses are given by Deer *et al.* (1963) and analysis 1 (table 56) shows a discrepancy of 7 % in the Mg ratio, the remainder lying on or very close to the curve (fig. 1, line 1). Since rapid colorimetric determinations of total iron on small quantities of material are easier to obtain than MgO values, they were carried out (by A. J. Easton) to estimate the Mg ratio of the unanalysed amphiboles; despite its yielding a less accurate value than that for MgO, the plot suggests an expected accuracy of within 5 %.

Similar curves for the richterite analyses in Deer *et al.* (1963) show rather better linearity for total iron (fig. 3, line 2) than for MgO (fig. 1, line 2). In the case of the glaucophane and riebeckite groups, for which separate curves were obtained, fair


● richterites (Deer *et al.*, 1963, table 55), ① eckermannitic asbestos, Colorado (Deer *et al.*, 1963, table 57, analysis 2), and ② eckermannite, Norra Kärr (Deer *et al.*, 1963, table 57), analysis 3. *Line 3*, glaucophanes and crossites, and *line 4*, riebeckite–magnesioriebeckite series; ● glaucophanes and crossites (Deer *et al.*, 1963, table 53), ○ riebeckite–magnesioriebeckite series (Deer *et al.*, 1963, table 54), ① eckermannitic asbestos, Colorado (Deer *et al.*, 1963, table 57, analysis 2), and ② eckermannite, Norra Kärr (Deer *et al.*, 1963, table 57, analysis 3). *Line 5*, kaersutites, *line 6*, basaltic hornblendes, and *line 7*, barkevikites; △ barkevikites (Deer *et al.*, 1963, table 51), ▲ basaltic hornblendes (Deer *et al.*, 1963, table 48), ● kaersutites (Deer *et al.*, 1963, table 50), and ○ kaersutite, minverite, Cornwall (Kempe, 1968a). *Lines 8, 9, and 10*, hornblendes; ● hornblendes (10) (Deer *et al.*, 1963, table 40), ▲ edenites and edenitic hornblendes (10) (Deer *et al.*, 1963, table 41), △ tschermakitic hornblendes (8) (Deer *et al.*, 1963, table 42), ○ pargasites, hastingsites, and ferrohastingsites (9) (Deer *et al.*, 1963, table 43). *Line 11*, ferroactinolite–actinolite–tremolite series (Deer *et al.* 1963, table 38). *Line 12*, ● grunerite–cummingtonite series (Deer *et al.*, 1963, table 36), and ○ tirodites (Bilgrami, 1955, table 1). FIG. 2 (right). Weight % MgO plotted against Mg ratio for all the analyses of monoclinic amphiboles given by Deer *et al.* (1963, tables 36, 38, 40, 41, 42, 43, 48, 50, 51, 53, 54, 55, 56, and 57); key as in fig. 1.

linear relationships were found for both MgO (fig. 1, lines 3 and 4) and total iron (fig. 3, lines 3 and 4).

In order to test the reliability of such plots further, MgO and total iron curves were obtained also for the dark brown hornblendes (basaltic hornblende and barkevikite form one curve, kaersutite a short, distinct one); the common hornblendes (for an Mg ratio of 40 upwards, hornblendes and edenites tend to form one curve; pargasites, hastingsites, and ferrohastingsites another; and tschermakitic hornblendes a third); the tremolite–actinolite series; and the cummingtonite–grunerite series. With two or three exceptions, there is remarkably little departure from linearity in these curves, which are given in figs. 1–4. For MgO, the common hornblendes (excepting tschermakitic hornblende) and the tremolite–actinolite series show apparent changes of slope at an Mg ratio of about 40 and 75, respectively, whilst the riebeckite curve changes slope abruptly at an Mg ratio of 40. The exceptions mentioned above are the overlapping of the hornblende–edenite group with the pargasite–hastingsite group; the presence of a distinct group of pargasite–hastingsite amphiboles, with Mg ratios between 70 and 80, which fall well below their curve, on that of glaucophane; and the Indian tirodites or manganiferous cummingtonites (Bilgrami, 1955; not given in Deer et al., 1963), which form a cluster well above the main cummingtonite–grunerite series (see below). The total iron curves show a similar relationship but there are few changes of slope or well-defined exceptions to linearity, whilst the common hornblendes do not fall so clearly into distinct groups.

The empirical curves of MgO and total iron plotted against Mg ratio are therefore useful in obtaining estimates of the compositions of amphiboles for which no analyses are available. They depend, of course, on the percentage of the metal cation sites occupied by the sum of Mg, Fe^{2+}, and Fe^{3+}, and on the number of such sites ($A+X+Y = 7$ to 8) in the structure of a particular amphibole group. The theoretical curves have been calculated, using a short computer programme written by Dr. M. H. Hey. The oxide percentages were computed for 5 % intervals of the Mg ratio in amphiboles of standardized composition, varying only in Mg:Fe^{2+} proportions, thus: $(A+X)_{n_1}(Mg,Fe^{2+})_{n_2}Fe^{3+}_{n_3}Al_{n_4}Ti_{n_5}Z_8O_{22}(OH)_2$, where Σn is from 7 to 8; n_1 from 0 to 3; n_2 from 3 to 7; n_3 from 0 to 2; n_4 from 0 to 2; and n_5 from 0 to 1. The curves, most of which are given (as dotted lines) in figs. 1 and 4, are not strictly linear, there being slight curvature due to the different equivalent weights of MgO and FeO (and Fe_2O_3). Agreement between theoretical and empirical curves is fair in most MgO plots, and especially so in the case of the grunerite–cummingtonite and actinolite–tremolite series, in which n_3, n_4, and n_5 are zero. The behaviour of the empirical riebeckite–magnesioriebeckite curve is notable; also the position of the Indian tirodites (Bilgrami, 1955) relative to the grunerite–cummingtonite curves. It suggests that the tirodites might be close to the magnesium end-member of the series, which so far has not been described.

In the case of total iron, the allocation of a fixed quantity of Fe_2O_3 renders the curves less accurate and this is seen especially in the case of the arfvedsonite–eckermannite and riebeckite–magnesioriebeckite series. Their high Fe_2O_3 content results in a close fit between the Li-rich amphiboles and the calculated curve.
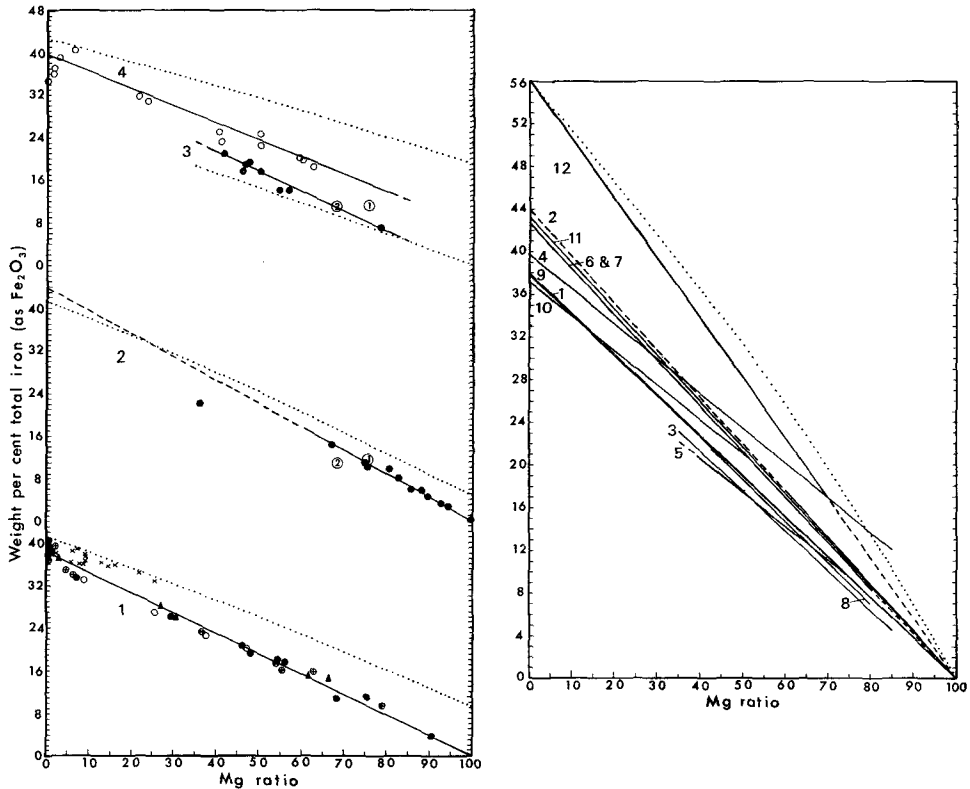
FIGS. 3 and 4. FIG. 3 (left). Weight % total iron (as Fe_2O_3) plotted against Mg or (Mg+Li) ratio for the analyses of various amphibole series given by Deer et al. (1963) and others. Where MnO exceeds 2 wt % it is included in (total) Fe_2O_3. The calculated curve is shown as a dotted line for each amphibole series. *Line 1*, arfvedsonite–eckermannite series and catophorites; ● arfvedsonite–eckermannite series (Deer et al., 1963, table 57), ◆ as above, including MnO, ▲ catophorites (Deer et al., 1963, table 56), ○ arfvedsonite–eckermannite series (Kempe and Deer, in press), △ catophorite (Kempe and Deer, in press), ✕ riebeckitic arfvedsonites (Borley, 1963, tables II and III), ⊗ magnesio-arfvedsonites (McKie, 1966, p. 279), and ⊕ others. *Line 2*, richterites; ● richterites (Deer et al., 1963, table 55), ◆ as above, including MnO, ① eckermannitic asbestos, Colorado (Deer et al., 1963, table 57, analysis 2), and ② eckermannite, Norra Kärr (Deer et al., 1963, table 57, analysis 3). *Line 3*, glaucophanes and crossites, and *line 4*, riebeckite–magnesioriebeckite series; ● glaucophanes and crossites (Deer et al., 1963, table 53), ○ riebeckite–magnesioriebeckite series (Deer et al. 1963, table 54), ① eckermannitic asbestos, Colorado (Deer et al., 1963, table 57, analysis 2), and ② eckermannite, Norra Kärr (Deer et al., table 57, analysis 3). FIG. 4 (right). Weight % total iron (as Fe_2O_3) plotted against Mg ratio for all the analyses of monoclinic amphiboles given by Deer et al. (1963, tables 36, 38, 40, 41, 42, 43, 48, 50, 51, 53, 54, 55, 56, and 57); key as in fig. 1. The calculated curve for the grunerite–cummingtonite series is shown as a dotted line.

Fair coverage of the arfvedsonite–eckermannite series was obtained up to an Mg ratio of about 60. Deer et al. (1963, table 57) give only three eckermannite analyses with Mg ratios higher than 60, two of which form the exceptions, mentioned above, from a linear relationship between MgO and total iron (wt %) and Mg ratio. The eckermannite with the highest ratio (90·6) is the emerald green 'szechenyiite' from the

jadeite rock at Tawmaw, Burma (table 57, analysis 1), which falls on both MgO and total iron curves. It is noteworthy that as the jadeite rock in the collections of the British Museum (Natural History) revealed only actinolite, the second of the two amphiboles present in the jadeite dyke, the cell dimensions of this mineral, with an Mg ratio of 82, estimated from its total iron content, were also determined and found to be closely similar to those of the 'széchenyiite'. It therefore seems probable that the two amphiboles are closely related. The eckermannite with the second highest Mg ratio (75·3), analysis 2, forms one exception to linear agreement between oxides and Mg ratio. This amphibole is asbestiform and falls on both richterite curves, and between both pairs of riebeckite and glaucophane curves, to which groups it may be related; it was not available for X-ray investigation. The third highest (Mg ratio: 68·1) amphibole comes from the kaxtorpite of Norra Kärr, Sweden (analysis 3) and is the second exception. It does, however, contain 1·15 % Li_2O, and falls below the (MgO+ Li_2O) curve; it also falls below the richterite MgO curve and lies practically on that of glaucophane. This amphibole should, perhaps, be in fact described as a glaucophane (Professor J. Zussman, personal communication). Its total iron is very slightly below the predicted value, whereas the Nigerian arfvedsonites fall above the iron curve. The Mg ratio includes Li, as for the Nigerian amphiboles; if Li is excluded the figure falls to 50·8. Two specimens of kaxtorpite are included in the British Museum collections and the cell parameters of the blue amphiboles from both have been determined, together with their total iron values. In the case of the first (BM 1949, 151) it was found that the cell dimensions were exceptionally low. This sample has an Mg ratio of 69, estimated from its total iron content, and an approximate Li_2O content of 0·95 %; its cell parameters are seen to fall on the extrapolated curves for the Nigerian Li-rich arfvedsonites, which, as described in the next section, are considerably lower than for the normal members of the series. It is therefore taken to correspond with the amphibole given in Deer et al. (1963, table 57, analysis 3). The second specimen (BM 1951, 408 (21)) has an estimated Mg ratio of 66, and a Li_2O determination gave 0·62 %. This specimen has the cell parameters to be expected from its Mg ratio, and is regarded either as a relatively Li-poor example of the same eckermannitic amphibole, or as corresponding to the second analysed amphibole recently separated from a specimen of the Norra Kärr rock by Dr. R. A. Howie (personal communication, 1968).

It may be noted that Li_2O is also present in the arfvedsonites of the Lovozero massif in quantities of up to 0·5 % (Vlasov et al., 1966); of the Yenisei Range, up to c. 0·7 % (Sveshnikova and Kalenchuk, 1962); and of the Kangerdlugssuaq alkaline intrusion (see table I), up to c. 0·1 %.

Little comment is required on the remaining six amphiboles for which the Mg ratio has been estimated from total iron content. They include a greyish-green to brown (in thin section) arfvedsonite from Khibina, Kola Peninsula (BM 1961, 236); a blue magnesio-arfvedsonite from Lulu Kop, Palabora, E. Transvaal (BM 1932, 104(2)); a blue magnesio-arfvedsonite from the Loyne Mass, Borolan Complex, Scotland, and two from fenites, from the Fen area, Norway, and Namangali, Malawi (provided by Dr. A. R. Woolley); and a red to violet manganoan arfvedsonite (juddite) from Chikla, India (BM 1955, 122). The latter has an estimated Mg ratio of 62, compared with that

of 54·2 for the specimen quoted in Deer *et al.* (1963, table 57, analysis 13). In estimating the Mg ratio for this specimen, MnO was included in the total iron; in all cases, a slightly displaced parallel curve in which MnO is included can be used for total iron. It is notable also that the juddite contains 0·88 % of Li_2O.

X-ray data. The cell parameters were determined by Philips diffractometer, using Cu- or Co-$K\alpha$ radiation, or by 11·46-cm diameter powder camera, using Co-$K\alpha$ radiation, or by both. Where both were used, it was found that the powder film values were slightly and systematically lower than those obtained by diffractometer, which is regarded as the more accurate method. For the diffractometer measurements, silicon was used as an internal standard and the 310 peak (and, in the case of the iron-rich arfvedsonites, the 510 peak, and in the magnesium-rich samples, the 480 peak) disregarded.

Preliminary indexing was carried out from the ASTM card (14–633) for arfvedsonite; an approximate set of cell parameters was then calculated by means of a least-squares computer programme (supplied by Dr. P. J. Woodrow), which were in turn used to generate a complete set of indices using an enumeration programme (supplied by Dr. R. J. Davis). The 2θ values were then reindexed and the cell parameters refined, the space group $C2/m$ being adopted throughout. In view of the great degree of ambiguity in indexing the higher angle reflections in a large unit cell, zero, first, and second layer c-axis Weissenberg photographs were taken and indexed, in order to eliminate impossible indices from amongst those enumerated. Third-layer reflections were all regarded as possible, since a c-axis Weissenberg photograph of the third-layer reflections could not be taken, although two impossible reflections of the type *hol*, with *l* odd, have been eliminated in view of the findings of Kawahara (1963).

In table II the full enumerated lists for an arfvedsonite and an eckermannite are given, up to 2θ (Cu-$K\alpha$) 45°, in order to demonstrate the degree of ambiguity encountered, with intensity, absence, or non-visibility noted from the Weissenberg photographs. The final indexed lists given have been used throughout, individual reflections of poor quality being omitted where necessary. The $\Delta 2\theta$ for observed and calculated values of the end-members are given in table III.

Several distinctive changes are apparent in the two lists of reflections, probably caused by structural variations, which also result in the change of position of the optic axial plane from its anomalous position, normal to (010), in arfvedsonites to the usual amphibole position, parallel to (010), in eckermannites. The most remarkable change is the absence in arfvedsonites of the 020 reflection, characteristic of all other amphiboles. This reflection is outside the field of the zero-layer Weissenberg photograph but is conspicuously absent in the preliminary rotation photograph. It appears in no. 22, at an Mg ratio of about 27. Also, at this point, the 11$\bar{1}$ reflection appears, its place in the iron-rich members having been taken by 200. The 200 reflection remains in most of the more magnesian examples but is generally weaker than the 11$\bar{1}$. Two reflections absent in the iron-rich members appear at an Mg ratio of about 50: 220 and 24$\bar{2}$. The latter, however, is also weakly present in no. 22 (Mg ratio, 27). Similarly, some reflections present in the iron-rich members (e.g. 55$\bar{1}$) are absent or extremely weak at the magnesian end of the series. In general, the magnesian members of the series show

TABLE II. *Possible hkl values enumerated for an arfvedsonite (no. 10) and an eckermannite (no. 33). Intensities (I) are from Weissenberg photographs. ab.: absent; n.v.: not visible*

Arfvedsonite				Eckermannite			
I	hkl	d (Å)	Indexed patterns	Indexed patterns	I	hkl	d (Å)
n.v.	020	9·0460	—	020	m	020	8·8445
s	110	8·4839	110	110	w	110	8·2982
n.v.	001	5·1635	—	—	n.v.	001	5·1201
m	130	5·1075	130	130	m	130	4·9944
ab.	$11\bar{1}$	4·8922	$11\bar{1}$	$11\bar{1}$	n.v.	$11\bar{1}$	4·8482
m	200	4·8028	200	200	m	200	4·6982
s	040	4·5230	040	—	ab.	021	4·4311
m	021	4·4844	—	040	s	040	4·4222
ab.	220	4·2420	220	220	m	220	4·1491
n.v.	111	4·0483	111	111	s	111	3·9907
m	$20\bar{1}$	4·0284	—	—	m	$20\bar{1}$	3·9777
m	$13\bar{1}$	3·8859	$13\bar{1}$	$13\bar{1}$	m	$13\bar{1}$	3·8317
w	$22\bar{1}$	3·6800	$22\bar{1}$	$22\bar{1}$	s	$22\bar{1}$	3·6277
s	131	3·4208	131	131	s	131	3·3641
m	041	3·4023	—	—	w	041	3·3467
w	150	3·3861	—	—	ab.	150	3·3109
s	240	3·2927	240	240	s	240	3·2201
ab.	201	3·1608	—	—	w	201	3·1054
s	310	3·1528	310	310	s	310	3·0841
m	$31\bar{1}$	3·0254	$31\bar{1}$	$31\bar{1}$	s	$31\bar{1}$	2·9761
w	060	3·0153	060	$24\bar{1}$	ab.	$24\bar{1}$	2·9574
m	$24\bar{1}$	3·0082	—	060	m	060	2·9482
s	221	2·9839	221	221	s	221	2·9300
w	$15\bar{1}$	2·9475	$15\bar{1}$	$15\bar{1}$	s	$15\bar{1}$	2·8959
s	330	2·8280	330	330	s	330	2·7661
m	$33\bar{1}$	2·7349	—	—	s	$33\bar{1}$	2·6873
s	151	2·7283	151	151	s	151	2·6775
s	$1\bar{1}2$	2·6290	—	—	s	$1\bar{1}2$	2·6095
s	061	2·6039	061	002	s	002	2·5600
m	241	2·5908	—	061	s	061	2·5549
s	002	2·5818	—	—	ab.	241	2·5414
w	260	2·5537	—	$20\bar{2}$	s	$20\bar{2}$	2·5206
s	$20\bar{2}$	2·5408	$20\bar{2}$	—	w	260	2·4972
m	170	2·4958	170	—	m	022	2·4591
ab.	022	2·4826	—	170	s	170	2·4403
w	311	2·4473	—	—	m	222	2·4241
ab.	222	2·4461	—	—	w	$13\bar{2}$	2·4082
m	$13\bar{2}$	2·4316	—	—	w	311	2·3997
m	$26\bar{1}$	2·4140	—	—	m	$26\bar{1}$	2·3685
ab.	$40\bar{1}$	2·4081	—	—	m	$40\bar{1}$	2·3645
m	400	2·4014	400	400	w	400	2·3491
m	350	2·3979	350	350	s	350	2·3451
s	$35\bar{1}$	2·3403	$35\bar{1}$	—	ab.	112	2·3103
m	112	2·3366	—	$35\bar{1}$	s	$35\bar{1}$	2·2965
s	$42\bar{1}$	2·3271	—	—	s	$42\bar{1}$	2·2842
ab.	420	2·3210	—	—	ab.	420	2·2704
m	$17\bar{1}$	2·3037	$17\bar{1}$	$17\bar{1}$	s	$17\bar{1}$	2·2591
w	331	2·2858	331	$31\bar{2}$	s	$31\bar{2}$	2·2532
s	$31\bar{2}$	2·2767	$31\bar{2}$	331	m	331	2·2405
w	080	2·2615	—	—	m	042	2·2156
ab.	042	2·2422	—	—	s	080	2·2111
s	$24\bar{2}$	2·2152	—	$24\bar{2}$	s	$24\bar{2}$	2·1899
ab.	132	2·1948	—	—	ab.	132	2·1672
s	171	2·1944	—	—	s	171	2·1507
s	261	2·1818	261	261	s	261	2·1381
s	$33\bar{2}$	2·1449	$33\bar{2}$	$33\bar{2}$	s	$33\bar{2}$	2·1198
m	$15\bar{2}$	2·1417	$15\bar{2}$	$15\bar{2}$	m	$15\bar{2}$	2·1150
w	$44\bar{1}$	2·1256	—	—	w	$44\bar{1}$	2·0851
ab.	440	2·1210	—	—	ab.	440	2·0746
s	202	2·0768	202	202	s	202	2·0481
w	081	2·0715	—	—	m	081	2·0299
ab.	280	2·0460	—	—	ab.	280	2·0006
s	351	2·0400	351	351	s	351	1·9986

the normal amphibole reflections, whilst the iron-rich arfvedsonites exhibit the differences. It should be noted, however, that Professor R. Sadanaga records very weak reflections ($I/I_0 = 2$ %) for both the 020 and 220 spacings for the arfvedsonite, no. 2 (Mg ratio, 1·1), described by Kawahara (1963) and given on the ASTM data card (14-633).

TABLE III. $\Delta 2\theta$ (i.e. $2\theta_{obs}-2\theta_{calc}$, Cu-$K\alpha$ radiation) for an arfvedsonite (no. 10; Arf.) and an eckermannite (no. 33; Eck.)

Arf. $\Delta 2\theta$	hkl	Eck. $\Delta 2\theta$	Arf. $\Delta 2\theta$	hkl	Eck. $\Delta 2\theta$	Arf. $\Delta 2\theta$	hkl	Eck. $\Delta 2\theta$
—	020	−0·017	0·006	240	0·022	—	24$\bar{2}$	0·000
−0·007	110	0·015	—	310	−0·019	0·002	261	−0·023
0·013	130	0·001	0·000	221	0·000	0·001	202	−0·001
−0·023	200	—	0·002	330	0·013	−0·010	351	—
0·013	040	−0·006	−0·010	151	—	0·011	421	—
0·024	111	0·003	0·003	061	0·009	−0·007	19$\bar{1}$	0·001
—	13$\bar{1}$	0·007	−0·006	20$\bar{2}$	0·002	−0·002	55$\bar{1}$	—
0·001	22$\bar{1}$	−0·019	0·011	35$\bar{1}$	—	−0·005	461	0·006
−0·003	131	0·015	0·015	17$\bar{1}$	—	—	480	−0·002

The cell parameters a, b, c, β, volume, and $a\sin\beta$ are given in table IV and fig. 5, separate curves being drawn for the Li-rich members, except for c and β. A tentative curve for b for the high-calcium amphiboles is also given. All parameters, especially a and b, are seen to decrease with increase of Mg ratio, signifying principally substitution of Mg (0·66 Å) for Fe^{2+}(0·74 Å). In the case of the Li-rich amphiboles, the decrease in b, especially, and therefore volume, and, to a lesser extent, a, and therefore $a\sin\beta$, appears very much greater.

In order to investigate the possible correlation between the chemistry of the amphiboles and their cell parameters, a multivariate analysis was carried out using the computer programme written by Hey (1969). Weighted data comprising 11 chemical and 4 physical variables, with their assessed probable errors, were used. Chemical: SiO_2, TiO_2 (including a value corrected for ZrO_2), Al_2O_3, Fe_2O_3, FeO (including ZnO and MnO), MgO, CaO, Na_2O (including K_2O), Li_2O, H_2O+, and F (including Cl). Physical: a, b, c, and β.

Unfortunately, the variations in β and in three of the chemical variables are only small; the standard deviations for Fe^{3+}, Na, OH, and β are only 4·2, 5·5, 2·8, and 4·6 times the assessed probable errors of their determinations respectively. A product-moment correlation matrix shows marked positive correlation (0·86) of the cell-sides a and b, medium correlation (0·67) of b and c, and weak correlation (0·40) of a and c; β appears to vary independently of the cell sides. Among the chemical variables there is a marked positive correlation (0·88) between Li and F, in agreement with Bowden (1966); there are also a number of marked correlations to be expected from the general amphibole formula and arising from the substitutions NaSi $\rightleftharpoons$ CaAl, Fe^{2+} $\rightleftharpoons$ Mg, and OH $\rightleftharpoons$ F, which will lead to instability in any equation of relation

TABLE IV. *Cell parameters of the arfvedsonite–eckermannite series and catophorites; mg, Mg or (Mg+Li) ratio*

No.	mg	a (Å)	b (Å)	c (Å)	β (°)	volume (Å)^3	$a \sin \beta$ (Å)
I	0·4	(9·894)	(18·090)	(5·310)	(103·95)	(922·5)	(9·602)
2	I·I	9·94	18·17	5·34	104·4	934·0	9·63
3	I·6	9·898	18·128	5·319	104·01	925·8	9·602
4	4·4	(9·902)	(18·109)	(5·341)	(104·57)	(926·9)	(9·584)
5	5·7	9·841	18·036	5·318	103·74	922·0	9·560
6	6·2	9·806	18·047	5·329	103·71	916·2	9·527
7	6·4	(9·881)	(18·083)	(5·319)	(104·17)	(921·6)	(9·580)
8	7·I	9·865	18·066	5·326	103·79	921·9	9·581
9	7·7	9·847	18·009	5·313	103·73	915·1	9·564
10	8·6	9·891	18·092	5·317	103·80	924·0	9·605
		(9·861)	(18·065)	(5·304)	(103·60)	(918·4)	(9·585)
II	8·7	9·837	18·014	5·321	103·71	916·1	9·557
12	8·8	9·839	18·087	5·334	103·78	921·9	9·556
13	8·9	9·824	18·061	5·332	103·77	918·9	9·542
14	8·9	9·830	18·015	5·319	103·71	915·1	9·550
15	12·6	9·837	18·033	5·321	103·68	917·1	9·558
16	14·I	9·824	18·006	5·320	103·74	914·0	9·542
17	15·8	9·825	17·995	5·321	103·79	913·7	9·542
18	(18)	9·964	18·078	5·323	104·29	929·2	9·656
		(9·941)	(18·051)	(5·313)	(104·24)	(924·1)	(9·636)
19	21·6	9·813	17·954	5·310	103·66	909·0	9·535
20	25·4	9·810	17·943	5·307	103·83	907·0	9·525
21	25·4	9·871	18·016	5·326	103·82	919·8	9·585
22	26·9	(9·884)	(18·136)	(5·293)	(104·26)	(919·5)	(9·579)
23	37·3	9·871	18·050	5·320	104·29	918·5	9·566
		(9·861)	(18·024)	(5·314)	(104·39)	(914·9)	(9·552)
24	46·9	(9·875)	(18·004)	(5·302)	(104·23)	(913·8)	(9·572)
25	(53)	(9·860)	(18·022)	(5·285)	(104·30)	(910·0)	(9·554)
26	55·2	(9·75)	(17·84)	(5·28)	(104·1)	(890·6)	(9·46)
27	(59)	9·865	18·075	5·282	104·61	911·4	9·546
		(9·819)	(17·971)	(5·276)	(104·39)	(901·7)	(9·511)
28	(59)	9·839	17·944	5·275	103·90	904·0	9·551
29	(62)	9·800	17·865	5·277	104·09	896·0	9·504
		(9·769)	(17·811)	(5·270)	(104·00)	(889·7)	(9·479)
30	62·7	9·859	17·954	5·287	104·13	907·5	9·561
		(9·833)	(17·900)	(5·272)	(104·18)	(899·6)	(9·533)
31	(66)	9·850	17·933	5·273	103·98	903·9	9·558
32	(66)	9·801	17·882	5·288	103·92	899·5	9·513
33	(69)	9·693	17·700	5·291	104·08	880·4	9·399
		(9·688)	(17·689)	(5·279)	(104·10)	(877·5)	(9·396)
34	78·9	(9·80)	(17·91)	(5·29)	(104·1)	(900·3)	(9·50)
35	(90·6)	9·855	17·884	5·272	104·18	900·9	9·552
Estimated accuracy (diffractometer determinations):		±0·01	±0·02	±0·01	±0·1	±2·0	±0·01

Parameters in parentheses denote determinations by 11·46 cm powder camera, regarded as of low accuracy.

Mg ratios in brackets are estimates from the (total) Fe_2O_3 *vs.* Mg ratio curve (fig. 3). The Mg ratio of no. 35 is that given by Deer *et al.* (1963, table 57, analysis 1).
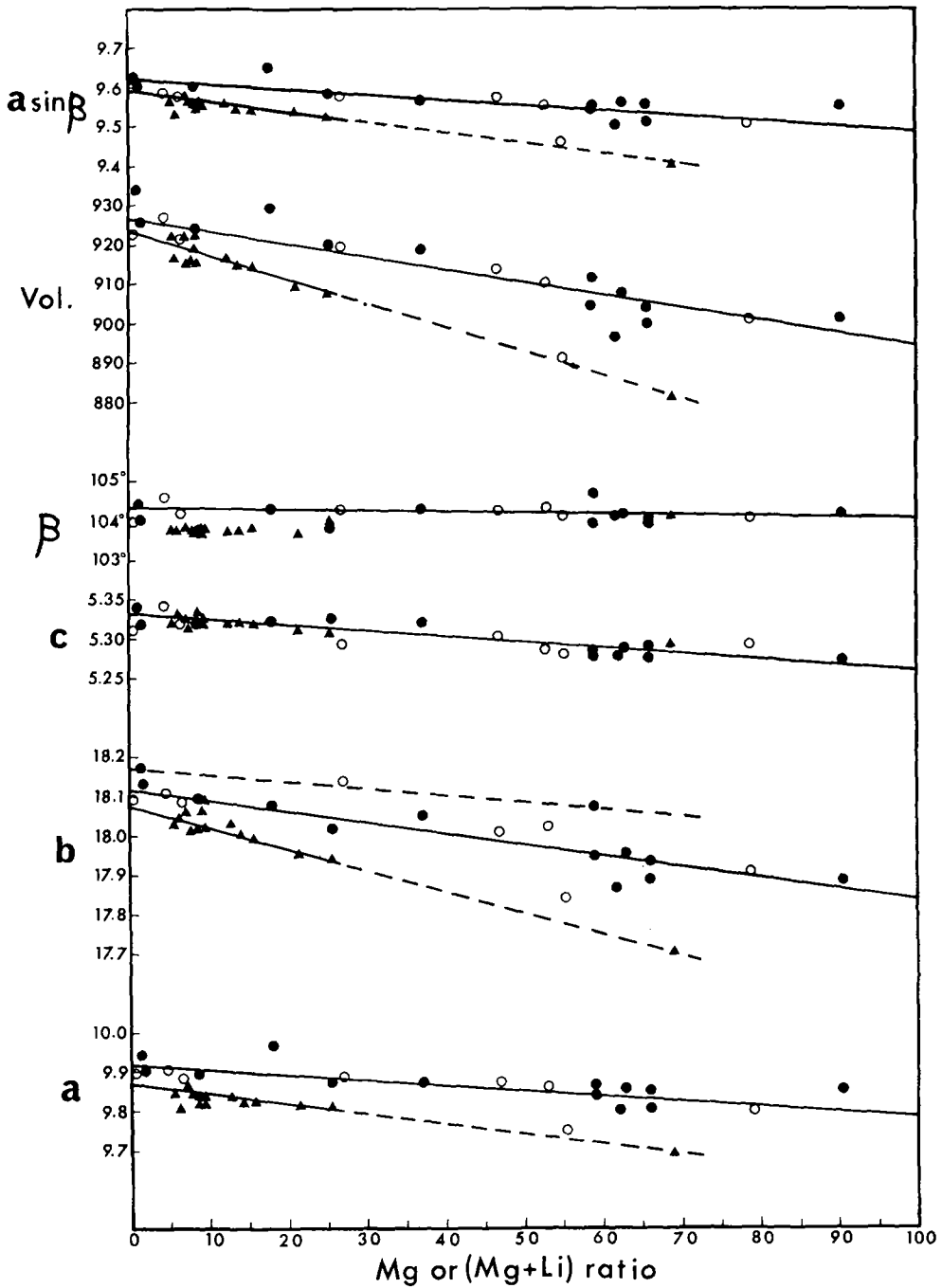
Fig. 5. Cell parameters for the arfvedsonite–eckermannite series and catophorites (a, b, c, β, volume and $a \sin \beta$), plotted against Mg or (Mg+Li) ratio. ● and ▲ values from diffractometer; ○ values from 11·46-cm powder camera. Circles, normal Li_2O content. Triangles, high Li_2O content, mainly from Frost (1963, table I). For b, upper dashed line indicates values for Ca-rich amphiboles, e.g. catophorites. Lower dashed lines indicate values for Li-rich amphiboles.

between the variables that includes both Na and Ca, Si and Al, Si and Ca, Fe^{2+} and Mg, or OH and F.

Since the condition $\Sigma(O,OH,F) = 24$ enables us to eliminate only one chemical variable, stable equations cannot be derived, but although many of the coefficients are statistically insignificant because of the correlations among the chemical variables, the equations reproduce the physical quantities satisfactorily within the range of

TABLE V. *Best-fit equations relating the cell-dimensions and compositions of 28 arfved-sonites and eckermannites (the specimens listed in table I, excluding nos. 18, 25, 27, 28, 29, 31, and 32, for which full chemical data were not available). The equations are in the form a* (or *b* or *c* or *β*) $= \alpha+\beta(Na-2)+\gamma(Ca-0\cdot5)+\delta Fe^{2+}+\epsilon Li+\zeta(Fe^{3+}-1\cdot5)+\eta Ti+\theta(Si-7\cdot5)+\iota(Al-0\cdot5)+\kappa(OH-2)+\lambda F$, *where the composition is in atoms per* $24(O,OH,F)$; *the standard error of each coefficient is tabulated below the coefficient, and that of the physical variable below* α

	α	β	γ	δ	ϵ	ζ
a	9·682 Å	0·244	0·420	0·044	0·027	0·021
	±0·079	±0·100	±0·200	±0·033	±0·106	±0·113
b	17·855 Å	0·123	0·300	0·078	0·034	0·037
	±0·055	±0·070	±0·138	±0·023	±0·074	±0·078
c	5·327 Å	−0·044	−0·095	0·007	−0·008	0·003
	±0·014	±0·018	±0·035	±0·006	±0·019	±0·020
β	103·31°	1·06	2·40	0·13	0·40	0·38
	±0·35	±0·45	±0·88	±0·15	±0·47	±0·50
		Na	Ca	Fe^{2+}	Li	Fe^{3+}

	η	θ	ι	κ	λ
a	−0·029	0·311	0·145	0·292	0·005
	±0·317	±0·232	±0·135	±0·077	±0·129
b	−0·032	0·180	0·054	0·197	−0·039
	±0·021	±0·162	±0·094	±0·054	±0·090
c	−0·061	−0·081	−0·034	−0·045	−0·004
	±0·056	±0·040	±0·024	±0·014	±0·023
β	0·70	2·32	1·39	1·28	−0·38
	±1·42	±1·04	±0·60	±0·34	±0·58
	Ti	Si	Al	OH	F

compositions studied. Equations were computed with elimination of Mg, of Si, or of Ti; since Fe^{2+} and Mg are the most strongly correlated pair of chemical variables, the equations with Mg eliminated are the most stable.

Table V gives the equations for the variations in the cell-dimensions with substitutions for Mg in a magnesio-arfvedsonite of composition

$$Na_2Ca_{0\cdot5}Mg_{3\cdot5}Fe^{3+}_{1\cdot5}Si_{7\cdot5}Al_{0\cdot5}O_{22}(OH)_2;$$
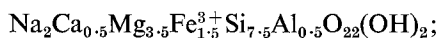
in these equations, the coefficients for the cations refer to theoretical valency-balanced substitutions (Na for 0·5 Mg, Al for 1·5 Mg, etc.) and those for OH and F to the substitutions OH or F for $Mg_{0\cdot5}O$. Since most of the substitutions actually encountered

are coupled, the effects of a selection of the most important coupled substitutions are given in table VI. Although many of the coefficients in table V are not statistically significant (the coefficient should be at least twice its standard error to be significant at the 5 % level), they show some suggestive regularities; more data, if possible over a wider field of compositions, are clearly desirable.

TABLE VI. *Effect of some substitutions on the cell-dimensions in the arfvedsonite-eckermannite series (derived from the equations of table V)*

	$Mg \rightarrow Fe^{2+}$	$Mg \rightarrow Ca$	$MgAl \rightarrow NaSi$	$2Mg \rightarrow LiFe^{3+}$	$MgTi \rightarrow 2Fe^{3+}$	$CaMg \rightarrow NaFe^{3+}$
a	0·044 Å	0·420	0·411	0·045	0·071	−0·156
b	0·078 Å	0·300	0·249	0·070	0·106	−0·141
c	0·007 Å	−0·095	−0·091	−0·005	0·068	0·054
β	0·13°	2·40	1·99	0·78	0·06	0·96

	$NaSi \rightarrow CaAl$	$OH \rightarrow F$	$Fe^{2+}OH \rightarrow Fe^{3+}O$	$MgSi \rightarrow 2Al$	$2Mg \rightarrow Ti$
a	0·010	−0·288	−0·316	−0·022	−0·029
b	0·052	−0·236	−0·237	−0·072	−0·032
c	−0·004	0·041	0·041	0·013	−0·061
β	0·41	−1·65	−1·02	0·47	0·70

It is interesting to note that most substitutions that effect an increase in a also increase b but decrease c, and vice versa, but the effect of any substitution on c is less than on a or b (with one doubtful exception, Ti and a vacancy for 2 Mg). The replacements having most effect are: Ca for Mg and NaSi for MgAl, which increase a, b, and β and decrease c; $Fe^{3+}O$ for $Fe^{2+}OH$ and F for OH, which have the opposite effect; and $NaFe^{3+}$ for CaMg, which decreases a and b and increases β as well as c. The replacement of Mg by Fe^{2+} has relatively little effect, but it is interesting to note that replacement of all the Mg in the above formula by Fe^{2+} has approximately the same percentage effect on a, b, and c as in the orthopyroxenes (cf. Howie, Smith, Stephenson, and Hey, 1969).

These conclusions are in general agreement with those of Frost (1963), who found Ca and Fe^{2+} to increase a, b, and β but not affect c; F was found to decrease all four parameters, high (Fe^{2+} +Al+Ti) to increase c, and high Li or Na to decrease b. The discrepancies in the reported effects of Fe^{2+}, Li, and Na are probably due to concomitant variations in other components masking the true effect of these elements in Frost's analysis of his data; thus high Li tends to be correlated with high F, Na, and Fe^{3+} and low Ca, and while we find the substitution of $LiFe^{3+}$ for 2Mg to increase b, the substitutions $NaFe^{3+}$ for CaMg, $Fe^{3+}O$ for $Fe^{2+}OH$, and F for OH all decrease b strongly.

This investigation illustrates the difficulty of relating cell dimensions to chemistry in the case of amphiboles of highly variable composition, as compared, for example, with the cummingtonite–grunerite series (Klein, 1964; Viswanathan and Ghose, 1965).

REFERENCES

BILGRAMI (S. A.), 1955. *Min. Mag.* **30**, 633 [M.A. **12**–503].

BORLEY (G. D.), 1963. Ibid. **33**, 358 [M.A. **16**–381].

BOWDEN (P.), 1966. *Geochimica Acta*, **30**, 555 [M.A. **17**–752].

BROCK (P. W. G.), GELLATLY (D. C.), and VON KNORRING (O.), 1964. *Min. Mag.* **33**, 1057 [M.A. **17**–78].

DEER (W. A.), HOWIE (R. A.), and ZUSSMAN (J.), 1963. *Rock-forming Minerals*, vol. 2. London (Longmans, Green).

HEY (M. H.), 1969. *Min. Mag.* **37**–83.

HOWIE (R. A.), SMITH (S. V.), STEPHENSON (D. A.), and HEY (M. H.), 1969. Ibid. **37**, 90.

KEMPE (D. R. C.), 1968a. Ibid. **36**, 874.

—— 1968b. Ibid. **36**–1167 [M.A. **20**–50].

—— and DEER (W. A.). *Medd. om Grønland*, in press.

FROST (M. T.), 1963. *Min. Mag.* **33**, 377 [M.A. **16**–381].

KAWAHARA (A.), 1963. *Min. Journ. [Japan]*, **4**, 30 [M.A. **17**–22].

KLEIN (C. JR.), 1964. *Amer. Min.* **49**, 963. [M.A. **17**–192].

McKIE (D.), 1966. In *Carbonatites* (ed. TUTTLE, O. F., and GITTINS, J.). John Wiley—Interscience, New York, p. 279.

NAYAK (V. K.) and NEUVONEN (K. J.), 1963. *Bull. Comm. géol. Finlande*, **212**, 27 [M.A. **16**–645].

SVESHNIKOVA (E. V.) and KALENCHUK (G. E.) [Свешникова (Е. В.) и Каленчук (Г. Е.)], 1962. *Geochemistry*, no. 12, 1190; transl. of Геохимия, 1055–1065 [M.A. **16**–632].

VISWANATHAN (K.) and GHOSE (S.), 1965. *Amer. Min.* **50**, 1106 [M.A. **17**–510].

VLASOV (K. A.), KUZ'MENKO (M. Z.), and ES'KOVA (E. M.), [Власов (К. А.), Кузменко (М. З.), и Еськова (Е. М.)] 1966. *The Lovozero Alkali Massif.* Edinburgh and London (Oliver and Boyd).